THE JOURNAL OF BIOLOGICAL CHEMISTRY VOL. 287, NO. 36, pp. 30781–30788, August 31, 2012

The Polarity Protein Partitioning-defective 1 (PAR-1) Regulates Dendritic Spine Morphogenesis through Phosphorylating Postsynaptic Density Protein 95 (PSD-95)*

Received for publication, February 8, 2012, and in revised form, July 16, 2012 Published, JBC Papers in Press, July 17, 2012, DOI 10.1074/jbc.M112.351452

Qian Wu[1], **Victoria L. DiBona**[1], **Laura P. Bernard, and Huaye Zhang**[2]

From the Department of Neuroscience and Cell Biology, UMDNJ-Robert Wood Johnson Medical School, Piscataway, New Jersey 08854

Background: Dendritic spines are sites of excitatory synaptic inputs and play an important role in cognitive functions.
Results: The polarity protein PAR-1 regulates spine morphogenesis through phosphorylating PSD-95 at Ser-561.
Conclusion: PAR-1 plays an important role in spine morphogenesis through PSD-95.
Significance: Our work identifies a novel pathway that regulates spine morphogenesis.

The polarity protein PAR-1 plays an essential role in many cellular contexts, including embryogenesis, asymmetric cell division, directional migration, and epithelial morphogenesis. Despite its known importance in different cellular processes, the role of PAR-1 in neuronal morphogenesis is less well understood. In particular, its role in the morphogenesis of dendritic spines, which are sites of excitatory synaptic inputs, has been unclear. Here, we show that PAR-1 is required for normal spine morphogenesis in hippocampal neurons. We further show that PAR-1 functions through phosphorylating the synaptic scaffolding protein PSD-95 in this process. Phosphorylation at a conserved serine residue in the KXGS motif in PSD-95 regulates spine morphogenesis, and a phosphomimetic mutant of this site can rescue the defects of kinase-dead PAR-1. Together, our findings uncover a role of PAR-1 in spine morphogenesis in hippocampal neurons through phosphorylating PSD-95.

Dendritic spines are specialized protrusions on neurons that receive most of the excitatory synaptic inputs in the mammalian brain. The morphogenesis and plasticity of spines are believed to play a key role in cognitive functions, as a number of neurological disorders are associated with changes in the number, size, and shape of dendritic spines (1, 2). Because spines are highly asymmetric structures, with synapses forming on the top of the spine head, it is likely that proteins regulating cell polarity are involved in this process. Indeed, we recently found that the PAR polarity complex, including PAR-3, PAR-6, and atypical PKC (aPKC),[3] is important for spine morphogenesis (3, 4). However, the role of other polarity proteins in this process has been unclear.

The polarity protein PAR-1, also known as microtubule affinity-regulating kinase (MARK), was originally identified during a screen in *C. elegans* for genes involved in the specification of the anterior-posterior body axis (5). PAR-1 is a serine/threonine kinase that is known to phosphorylate microtubule-associated proteins (MAPs) (6). Phosphorylation of MAPs decreases their affinity for microtubules, which underlies the ability of PAR-1 to regulate microtubule dynamics and stability (7). In mammals, there are four members of the PAR-1 family, MARK1–4. Numerous studies have pointed to a key role for MARK/PAR-1 family members in regulating microtubule dynamics and polarity establishment in various cellular contexts (8). PAR-1 functions by phosphorylating a variety of substrates, including MAPs, Dishevelled, and histone deacetylase (9). Interestingly, MARK2/PAR-1b knock-out mice exhibit defects in spatial learning and memory (10). Furthermore, MARK1/PAR-1c is overexpressed in certain brain regions of autistic patients (11). These findings strongly support a role for PAR-1 in regulating cognitive functions of the brain. However, the underlying molecular and cellular mechanisms have been unclear.

In this study, we show that PAR-1 depletion causes defects in spine morphogenesis in hippocampal neurons and that a critical level of PAR-1 kinase activity is important for this process. Interestingly, although PAR-1 is known to regulate microtubule dynamics through phosphorylating MAPs, depletion of PAR-1 did not grossly affect microtubule transport. Instead, we found that PAR-1 functions through phosphorylating the synaptic scaffolding protein PSD-95. We found that PAR-1 phosphorylates PSD-95 at Ser-561 and that mutating this site to alanine reduces spine formation. In addition, a phosphomimetic mutant of PSD-95 was able to rescue the defects of kinase-dead PAR-1 in spine formation, suggesting that PAR-1 functions through PSD-95 in this process. Taken together, these results show a key role for PAR-1 in spine morphogenesis through phosphorylating PSD-95.

EXPERIMENTAL PROCEDURES

Plasmids—For knockdown of MARK1/PAR-1c, the following oligonucleotides against different regions of rat MARK1

* This work was supported, in whole or in part, by National Institutes of Health Grant NS065183 (to H. Z.). This work was also supported by a National Alliance for Research on Schizophrenia and Depression (NARSAD) Young Investigator Award (to H. Z.).

[1] Both authors contributed equally to this work.
[2] To whom correspondence should be addressed: Dept. of Neuroscience and Cell Biology, UMDNJ-Robert Wood Johnson Medical School, 675 Hoes Lane West, Piscataway, NJ 08854. Tel.: 732-235-3433; Fax: 732-235-4029; E-mail: zhang29@umdnj.edu.

[3] The abbreviations used are: aPKC, atypical PKC; MARK, microtubule affinity-regulating kinase; MAP, microtubule-associated protein; DIV, days *in vitro*.

were synthesized, annealed, and ligated into pSUPER and pSUPER-GFP vectors: PAR-1c shRNA1, 5′-gatccccGGATATACTGAAACGCATAttcaagagaTATGCGTTTCAGTATATCCttttttggaaa-3′ (forward) and 5′-agcttttccaaaaaGGATATACTGAAACGCATAtctcttgaaTATGCGTTTCAGTATATCCggg-3′ (reverse); PAR-1c shRNA2, 5′-gatccccGCAAATAATGAAAGACCGAttcaagagaTCGGTCTTTCATTATTTGCttttttggaaa-3′ (forward) and 5′-agcttttccaaaaaGCAAATAATGAAAGACCGAtctcttgaaTCGGTCTTTCATTATTTGCggg-3′ (reverse); and PAR-1c shRNA3, 5′-gatccccGGACCCAAGTGAAGGCGAAttcaagagaTTCGCCTTCACTTGGGTCCttttttggaaa-3′ (forward) and 5′-agcttttccaaaaaGGACCCAAGTGAAGGCGAAtctcttgaaTTCGCCTTCACTTGGGTCCggg-3′ (reverse). For knockdown of MARK2/PAR-1b, the following oligonucleotides against different regions of rat MARK2 were synthesized, annealed, and ligated into pSUPER and pSUPER-GFP vectors: PAR-1b shRNA1, 5′-gatccccGAGGTAGCTGTGAAGATCAttcaagagaTGATCTTCACAGCTACCTCttttttggaaa-3′ (forward) and 5′-agcttttccaaaaaGAGGTAGCTGTGAAGATCAtctcttgaaTGATCTTCACAGCTACCTCggg-3′ (reverse); and PAR-1b shRNA2, 5′-gatccccGAATGAACCTGAAAGCAAAttcaagagaTTTGCTTTCAGGTTCATTCttttttggaaa-3′ (forward) and 5′-agcttttccaaaaaGAATGAACCTGAAAGCAAAtctcttgaaTTTGCTTTCAGGTTCATTCggg-3′ (reverse). For expression of shRNAs in lentiviral vectors, the DNA fragment containing the shRNA-expressing oligonucleotide and the H1 RNA promoter from pSUPER was ligated into the pLVTHM vector (12).

The Myc-tagged human MARK1/PAR-1c construct was purchased from OriGene (Rockville, MD). The Myc- and Venus-tagged human MARK2/PAR-1b constructs were generously provided by Dr. Ian Macara (University of Virginia). The GW1-PSD-95-GFP construct was a generous gift from Dr. Ann Marie Craig (University of British Columbia). The S561A and S561D mutants of PSD-95 were generated by site-directed mutagenesis using GW1-PSD-95-GFP as the template. For construction of mitochondrially targeted monomeric red fluorescent protein, we obtained mitochondrially targeted photoactivatable GFP (Addgene plasmid 23348) from Dr. Richard Youle (NINDS, National Institutes of Health) (13). Photoactivatable GFP was removed from the construct, and a DNA fragment encoding monomeric red fluorescent protein was ligated downstream of the mitochondrial targeting sequence.

Neuronal Culture and Transfections—Hippocampal neuron cultures were prepared from embryonic rats as described previously (3). Briefly, hippocampuses were dissected from embryonic day 18 Sprague-Dawley rats, trypsinized, and triturated through a glass Pasteur pipette. Dissociated neurons were plated on glass coverslips coated with 1 mg/ml poly-L-lysine. After initial attachment, the coverslips were transferred to dishes containing a monolayer of glial cells. Cultures were grown in Neurobasal medium (Invitrogen) supplemented with B-27 (Invitrogen) and 2 mM GlutaMAX (Invitrogen). Neurons were transfected using either a CalPhos mammalian transfection kit (Clontech) or Effectene transfection reagent (Qiagen). For shRNA knockdowns, neurons were transfected at 11 days *in vitro* (DIV) and imaged at DIV14. For overexpression experiments, neurons were transfected at DIV5–6 and imaged at DIV17.

In Vitro Kinase Assay—The SH3 (Src homology 3) and guanylate kinase domains of wild-type PSD-95 and PSD-95(S561A) were subcloned into the pGEX4T-1 vector. GST fusion proteins were purified using glutathione-Sepharose beads (GE Healthcare) according to manufacturer's instructions. Myc-tagged PAR-1b constructs were expressed in HEK293FT cells, purified on Dynabeads® Protein G (Invitrogen), and served as the kinase source. For the kinase assay, purified GST fusion proteins (1 μg) were incubated with purified PAR-1 constructs in kinase buffer (25 mM Hepes, 25 mM β-glycerophosphate, 10 mM $MgCl_2$, 1 mM DTT, and 1 mM ATP) for 1 h at 30 °C. The reaction was stopped by adding 1× Laemmli sample buffer and analyzed by SDS-PAGE and Western blotting. Myc-PAR-1b constructs were eluted from the beads using 2× Laemmli sample buffer and analyzed by Western blotting. For denaturing conditions, HEK293 cell lysates expressing the Myc-PAR-1b constructs were incubated at 50 °C for 30 min before immunoprecipitation using Dynabeads Protein G.

Co-immunoprecipitation and Western Blotting—For co-immunoprecipitation experiments, HEK293 cells expressing different plasmid constructs were lysed on ice in buffer containing 25 mM Hepes, 150 mM NaCl, 10 mM $MgCl_2$, 1% Nonidet P-40, and 10 mM DTT and supplemented with protease inhibitor mixture (Sigma-Aldrich), phosphatase inhibitor mixture (Sigma-Aldrich), 10 mM β-glycerophosphate, and 10 mM NaF. Lysates were cleared by centrifugation at 13,000 × *g* for 10 min at 4 °C. Cleared lysates were incubated with anti-Myc monoclonal antibody 9E10 (2 μg) for 1 h at 4 °C, followed by incubation with 20 μl of Dynabeads Protein G preblocked with 5% BSA in lysis buffer. Beads were washed three times with lysis buffer. Bound proteins were eluted with 3× Laemmli sample buffer and subjected to SDS-PAGE and Western blot analysis.

For Western blot analysis, the primary antibodies used were rabbit anti-Myc antibody (1:2000; A-14, Santa Cruz Biotechnology, Santa Cruz, CA), rabbit anti-GFP antibody (1:4000; a generous gift from Dr. Ian Macara), and anti-rabbit phosphoserine antibody (1:1000; Abcam, Cambridge, MA). Horseradish peroxidase-conjugated goat anti-rabbit antibody (Jackson ImmunoResearch Laboratories, West Grove, PA) was used at 1:10,000 dilution. Proteins were visualized by enhanced chemiluminescence and imaged using a Syngene G:BOX iChemi XR system and GeneSnap software (Version 7.09.a; Syngene USA, Frederick, MD).

Immunocytochemistry—Hippocampal neurons were fixed in 4% paraformaldehyde with 4% sucrose in PBS for 15 min at room temperature. They were then either mounted for visualization of GFP or further processed for immunocytochemistry. For immunocytochemistry, fixed neurons were permeabilized with 0.2% Triton X-100 in PBS for 5 min at room temperature. Neurons were blocked with 20% goat serum in PBS for 1 h at room temperature and then incubated with primary antibodies diluted in 5% goat serum in PBS for 1 h at room temperature or overnight at 4 °C. Following washes with PBS, Alexa Fluor 594-conjugated secondary antibodies (Invitrogen) diluted in 5% goat serum were incubated with the neurons at room temperature for 1 h. Neurons were then washed with PBS and mounted using VECTASHIELD (Vector Laboratories, Burlingame, CA).

Microscopy and Image Quantification—Fluorescence images were acquired using an Olympus FV1000 confocal microscope with a 60× water immersion lens (numerical aperture of 1.00) or a Leica DMRE microscope with a 63× oil immersion lens (Plan Fluorite, numerical aperture of 1.25) coupled to a Hamamatsu ORCA-ER camera controlled by OpenLab software (Improvision, Boston, MA). Dendritic spine morphology and density were quantified by two individuals who were blind to the experimental conditions, and the results were averaged. Dendritic spines were defined as stubby or mushroom-shaped protrusions and contacted by presynaptic terminals. Filopodia were defined as long thin protrusions without an enlarged spine head and not contacted by presynaptic terminals. Spine density was measured by counting the number of spines on 80–100 primary and secondary dendrites from 15–20 neurons for each condition. Spine length and width were measured using ImageJ. Spine length was defined as the length from the tip of the spine head to the point where the spine joins the dendrite. Spine width was defined as the maximal width of the spine head perpendicular to the long axis of the spine neck. 250–400 spines from at least 15 neurons were measured for each condition. All experiments were repeated at least three times. A two-tailed, two-sample, unequal variance Student's *t* test was used to calculate the *p* values. *Error bars* represent the S.D. of the samples.

RESULTS

PAR-1 Kinase Activity Is Essential for Spine Morphogenesis—Our previous studies showed that the PAR-3·PAR-6·aPKC complex plays an essential role in dendritic spine morphogenesis. Interestingly, the proteins in this complex function through two different pathways. Although PAR-3 functions through the Rac exchange factor TIAM1 (3), PAR-6 and aPKC function through p190 RhoGAP and the RhoA GTPase (4). However, whether other PAR polarity proteins are involved in this process is unclear. To see if PAR-1 plays a role in spine morphogenesis, we began by depleting endogenous PAR-1 in cultured hippocampal neurons using shRNAs. We chose to deplete the MARK1/PAR-1c and MARK2/PAR-1b family members because of their high expression levels in the brain (6). In addition, MARK1/PAR-1c has been implicated in autism (11). shRNAs were introduced into neurons either through the pSUPER vector or through viral infections using a lentiviral vector. The efficiencies of the shRNAs were confirmed by RT-PCR and Western blotting (Fig. 1, *a* and *b*). PAR-1b shRNA1 and PAR-1c shRNA3 caused the most efficient depletion of their target proteins and were used in subsequent experiments. To visualize spine morphology, we used the pSUPER-GFP vector, which expresses both the GFP transgene and the shRNA. As shown in Fig. 1*c*, expression of MARK2/PAR-1b shRNA1 caused a spine dysgenesis phenotype in which the spines were elongated with smaller spine heads. Similar results were obtained with PAR-1b shRNA2 (data not shown). The mean length of spines was 2.10 ± 0.74 μm in PAR-1b knockdown neurons *versus* 0.96 ± 0.31 μm in control neurons. The mean width of spines was 0.48 ± 0.21 μm in PAR-1b knockdown neurons *versus* 0.75 ± 0.29 μm in control neurons ($p < 0.001$ for spine length and width compared with control neurons) (Fig. 1, *e* and *f*). Expression of MARK1/PAR-1c shRNA3 caused a similar but somewhat stronger phenotype in which most of the dendritic protrusions were filopodium-like with no head enlargement (Fig. 1, *c* and *d*). Quantification showed that the average spine width in PAR-1c knockdown neurons was 0.32 ± 0.10 μm (Fig. 1*h*), suggesting that PAR-1c depletion causes more prominent dysgenesis of the spine head ($p < 0.001$ for spine length and width compared with control neurons). Similar results were obtained with PAR-1c shRNA2 (data not shown). To see whether PAR-1b and PAR-1c might compensate for each other's function, we performed cross-rescue experiments in which we depleted one family member and rescued with the other member. Both PAR-1b and PAR-1c could efficiently rescue the defects caused by the loss of the other family member ($p < 0.001$ compared with knockdown neurons) (Fig. 1, *c* and *e–h*), suggesting that they play similar functions. In addition, when we depleted both PAR-1b and PAR-1c, we observed an even stronger phenotype in which the neurons showed smooth dendrites with a decreased number of protrusions compared with either knockdown alone (Fig. 1, *c* and *d*). This suggests that a "critical mass" of PAR-1 is necessary for spine morphogenesis. Depletion of one PAR-1 family member is sufficient to cause spine defects, the severity of which likely depends on the relative abundance of the family member, and depletion of both PAR-1b and PAR-1c causes an additive effect on the phenotype.

Next, we wanted to examine whether the kinase activity of PAR-1 is necessary for spine morphogenesis. To test this, we expressed kinase-dead PAR-1b (PAR-1b(T175A,S179A)) in PAR-1c-depleted neurons. Unlike wild-type PAR-1b, kinase-dead PAR-1b was unable to rescue the spine formation defects (Fig. 1, *c*, *g*, and *h*). Similar results were obtained when kinase-dead PAR-1c was expressed in PAR-1b-depleted neurons (data not shown). This shows that the kinase activity of PAR-1 is necessary for spine morphogenesis.

To further establish a role for PAR-1 kinase activity in spine morphogenesis, we overexpressed different PAR-1b mutants in neurons. When we expressed the kinase-dead PAR-1b(T175A,S179A) mutant in hippocampal neurons, we observed a significant decrease in the density of dendritic spines compared with control neurons expressing an empty vector (Fig. 2). Interestingly, a significant decrease in spine density was also observed in neurons overexpressing wild-type PAR-1b (Fig. 2). This suggests that a critical level of PAR-1 kinase activity is essential for proper spine morphogenesis. To further test this, we expressed PAR-1b constructs with Thr-562 mutated. The Thr-562 site is phosphorylated by aPKC, which inactivates PAR-1 (14, 15). Thus, the T562E mutant is an inactivated version of PAR-1b, whereas the T562A mutant is active. Both mutants showed a significant decrease in spine density compared with control neurons (Fig. 2), which further shows that the level of PAR-1 kinase activity is critical for spine morphogenesis and that either too much or too little PAR-1 kinase activity is detrimental. Taken together, these results show that PAR-1 plays an important role in spine morphogenesis and that a critical level of its kinase activity is necessary for this process.

PAR-1 Phosphorylates PSD-95 at Ser-561—Our next goal was to elucidate the mechanisms by which PAR-1 regulates spine morphogenesis. PAR-1 is known to phosphorylate

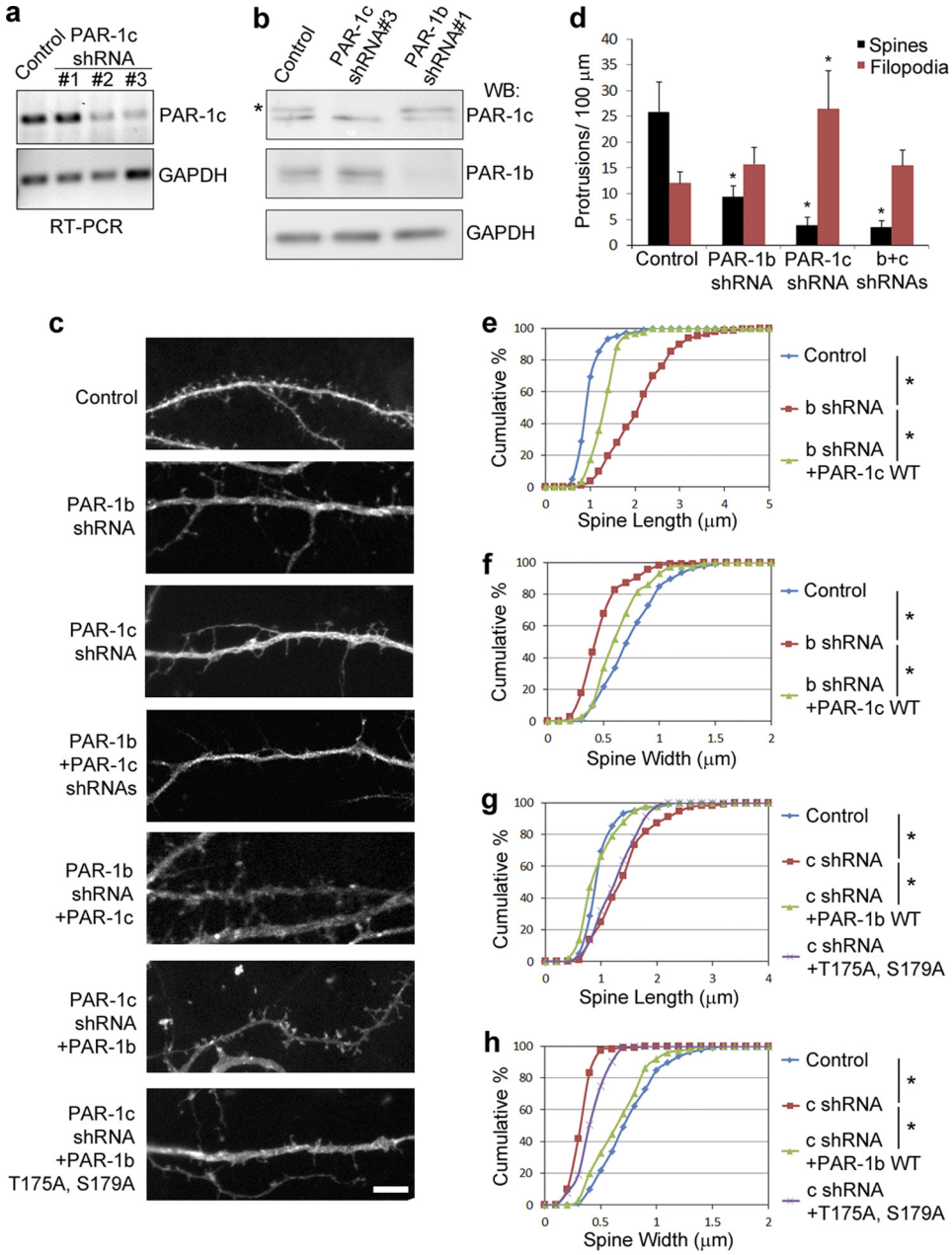

FIGURE 1. **PAR-1 kinase activity is necessary for spine morphogenesis.** *a*, cortical neurons were infected with lentivirus expressing an shRNA targeting luciferase (control) or the PAR-1c shRNA constructs. 72 h after infection, neurons were lysed, and total RNA was extracted. RT-PCR was performed to show the effectiveness of PAR-1c shRNAs in neurons. *b*, cortical neurons were infected with lentivirus expressing an shRNA targeting luciferase (control), PAR-1c shRNA3, or PAR-1b shRNA1. Neurons were lysed and subjected to Western blot (*WB*) analysis. Both PAR-1c shRNA3 and PAR-1b shRNA1 caused a >90% reduction in the expression of the targeted protein without affecting the other family member. The *asterisk* indicates the PAR-1c band. The *lower band* in the PAR-1c blot is likely a nonspecific band recognizing either another PAR-1 family member or an unrelated protein. It is unlikely to be a PAR-1c isoform because all known rat PAR-1c isoforms are identical in the region targeted by the shRNA. *c*, hippocampal neurons were transfected with luciferase shRNA (control) or the indicated shRNA and rescue constructs at DIV11, fixed, and imaged at DIV14. Depletion of PAR-1b caused a spine dysgenesis phenotype in which the spines were longer and thinner than those of the control neurons. Depletion of PAR-1c caused further dysgenesis of the spine head so that most of the protrusions lacked enlarged spine heads. The effect of PAR-1b depletion could be rescued by coexpressing wild-type PAR-1c. The effect of PAR-1c depletion could be rescued by coexpressing wild-type PAR-1b, but not kinase-dead PAR-1b(T175A,S179A). *Scale bar* = 5 μm. *d*, quantification of protrusion density. Spines were defined as stubby or mushroom-shaped protrusions with enlarged spine heads and contacted by presynaptic terminals. Filopodia were defined as long thin protrusions with no head enlargement and not contacted by presynaptic terminals. *, $p < 0.001$ compared with control neurons. *Error bars* represent S.D. of the samples ($n \geq 87$ for each condition). *e*, quantification of spine length under PAR-1b (*b*) knockdown and rescue conditions. *, $p < 0.001$ by Student's *t* test ($n \geq 306$ for each condition). *f*, quantification of spine width under PAR-1b knockdown and rescue conditions. *, $p < 0.001$ by Student's *t* test ($n \geq 260$ for each condition). *g*, quantification of spine length under PAR-1c (*c*) knockdown and rescue conditions. *, $p < 0.001$ by Student's *t* test ($n \geq 315$ for each condition). *h*, quantification of spine width under PAR-1c knockdown and rescue conditions. *, $p < 0.001$ by Student's *t* test ($n \geq 294$ for each condition).

MAPs and affect their affinity for microtubules, which in turn regulates vesicular transport along microtubules (16). We wondered whether the effect of PAR-1 is due to changes in microtubule transport. To test this, we expressed a mitochondrially targeted monomeric red fluorescent protein construct in either control or PAR-1c-depleted neurons. Mitochondrial distribution along the dendrites was not significantly different in these neurons (data not shown), sug-

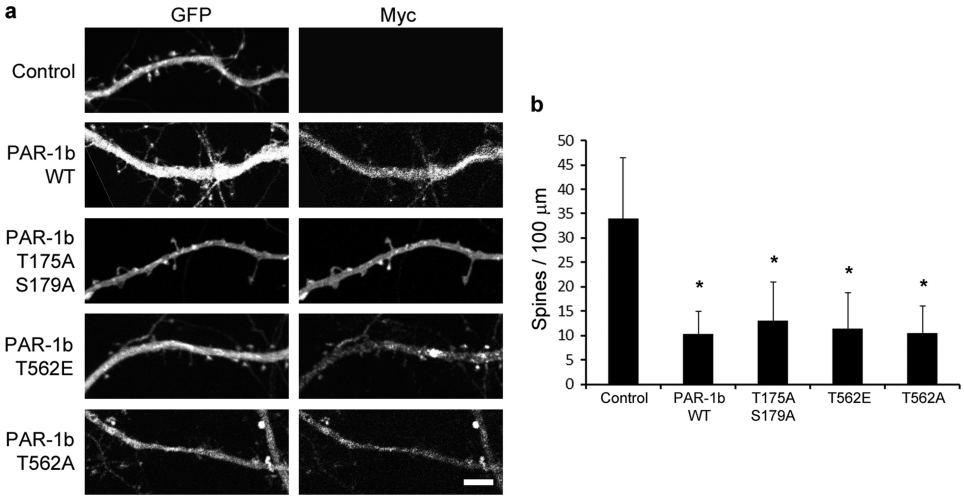

FIGURE 2. **Critical level of PAR-1 kinase activity is necessary for spine morphogenesis.** *a*, hippocampal neurons were transfected with different Myc-tagged PAR-1b constructs at DIV5–6, fixed, and imaged at DIV17. GFP was coexpressed to visualize spine morphology. Overexpression of both the active and inactive PAR-1b constructs caused a reduction in spine density, suggesting that a critical level of the kinase activity is necessary for spine morphogenesis. *Scale bar* = 5 μm. *b*, quantification of spine density of neurons in *a*. *, $p < 0.001$ by Student's *t* test. *Error bars* represent S.D. of the samples ($n \geq 81$ for each condition).

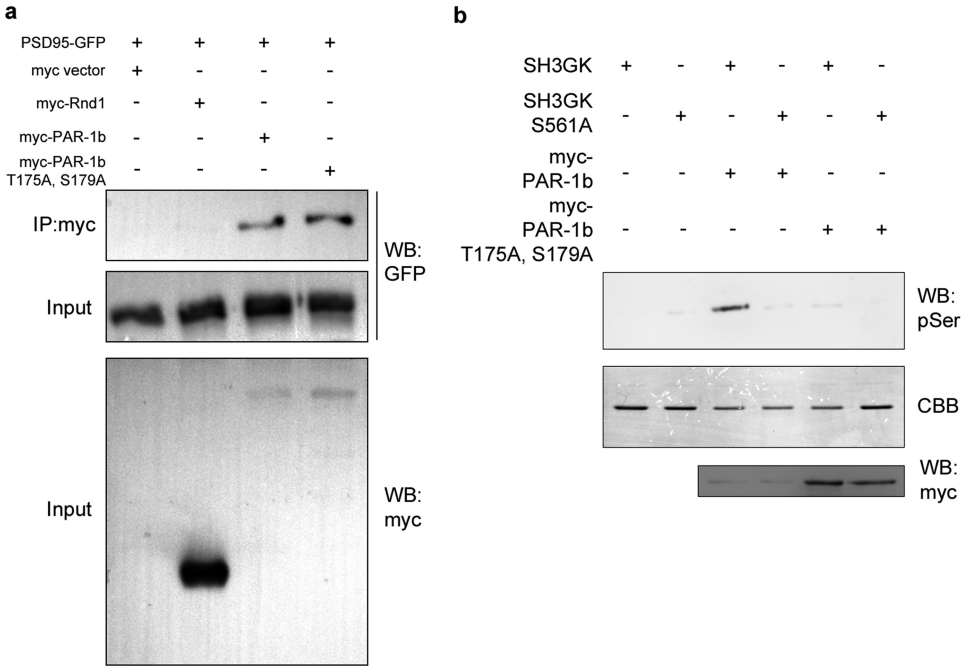

FIGURE 3. **PAR-1 phosphorylates PSD-95 at Ser-561.** *a*, PAR-1 interacts with PSD-95. HEK293 cells were transfected with the indicated constructs. Cell lysates were immunoprecipitated (*IP*) with anti-Myc antibody. Immunoprecipitated complexes were analyzed by Western blotting (*WB*). *b*, *in vitro* kinase assay showing the phosphorylation of wild-type PSD-95, but not the S561A mutant, by PAR-1. *Upper panel*, serine phosphorylation (*pSer*) was revealed by Western blotting using anti-rabbit phosphoserine antibody. *Middle panel*, Coomassie Brilliant Blue (*CBB*)-stained SDS-polyacrylamide gel showing total protein loading. *Lower panel*, expression of PAR-1b constructs was confirmed by Western blotting with anti-Myc antibody. *SH3GK*, SH3 and guanylate kinase domains.

gesting that PAR-1c depletion does not grossly affect microtubule transport.

We then hypothesized that PAR-1 regulates spine morphogenesis by phosphorylating a synaptic protein. Sequence analysis showed that there is a conserved serine (Ser-561) in the guanylate kinase domain of PSD-95 that matches the K*X*GS motif for PAR-1 substrates. Interestingly, Dlg, the *Drosophila* homolog of PSD-95, is phosphorylated by dPAR-1, the *Drosophila* homolog of PAR-1 (17). To see if PAR-1 might function through PSD-95, we first performed co-immunoprecipitation to examine the interaction between PAR-1 and PSD-95. Both wild-type and kinase-dead PAR-1b, but not an unrelated protein, were able to interact with PSD-95 (Fig. 3*a*), suggesting that PAR-1 might function by interacting with and phosphorylating PSD-95.

Next, we wanted to examine whether PAR-1 functions by phosphorylating PSD-95 at Ser-561. To test this, we performed an *in vitro* kinase assay. Wild-type PAR-1b or kinase-dead PAR-1b(T175A,S179A) was overexpressed in HEK293 cells, immunoprecipitated onto Protein G magnetic beads, and used as the kinase source. For substrates, we used purified GST fusion proteins of the SH3 and guanylate kinase domains of PSD-95 with or without the S561A mutation. As shown in Fig. 3*b*, robust serine phosphorylation was observed when wild-type PAR-1b was incubated with the wild-type SH3 and guanylate kinase

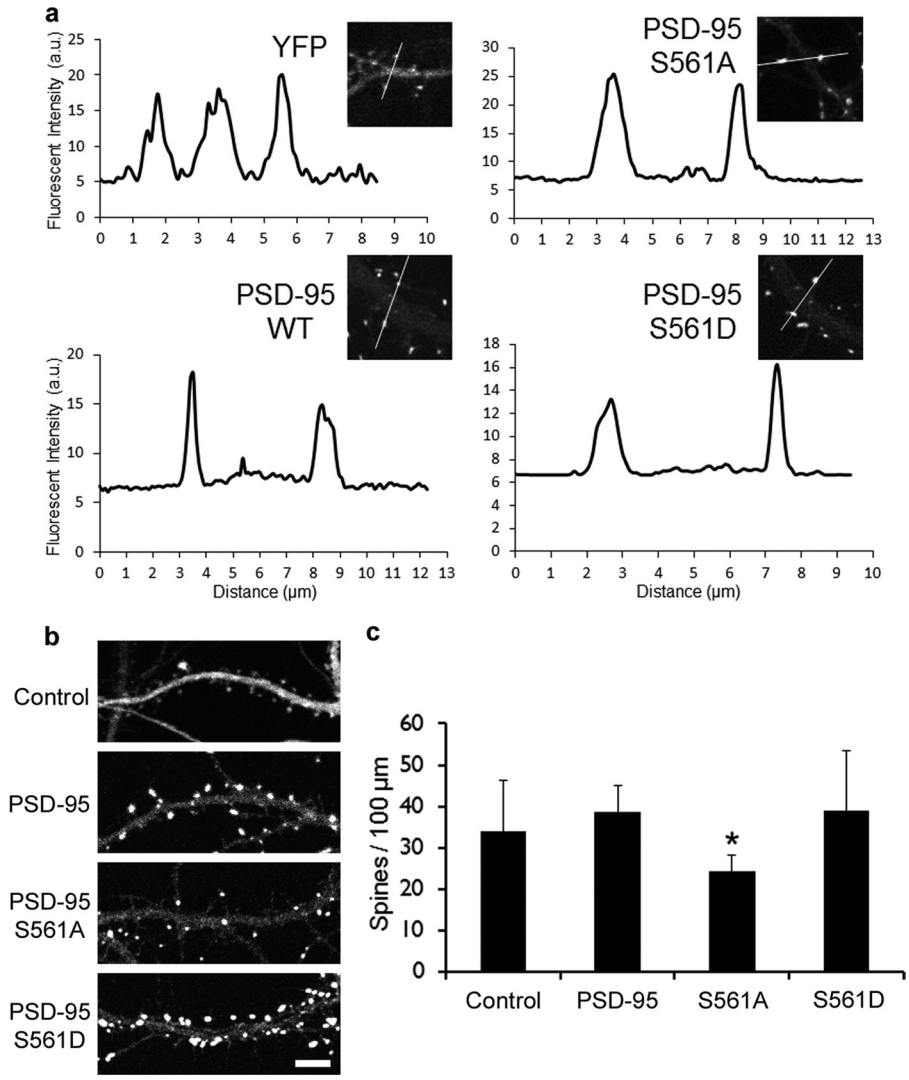

FIGURE 4. **Phosphorylation of PSD-95 at Ser-561 regulates spine morphogenesis.** *a*, phosphorylation at Ser-561 does not affect PSD-95 targeting to dendritic spines. Hippocampal neurons were transfected with the indicated constructs. Localization of each construct was examined by drawing a line across the dendrite and plotting the fluorescence intensity profile along the line. *a.u.*, arbitrary units. *b*, hippocampal neurons overexpressing different PSD-95 constructs were imaged at DIV17. PSD-95(S561A) caused a significant reduction in spine density compared with control neurons or neurons expressing PSD-95 (wild-type or S561D) constructs. *Scale bar* = 5 μm. *c*, quantification of spine density in neurons shown in *b*. *, $p < 0.001$ by Student's *t* test. *Error bars* represent S.D. of the samples ($n \geq 98$ for each condition).

domains, but not with the S561A mutant. Furthermore, minimal phosphorylation was observed when kinase-dead PAR-1b was used as the kinase source (Fig. 3*b*) or when PAR-1b was denatured (data not shown). This suggests that PAR-1 can phosphorylate PSD-95 at Ser-561.

Ser-561 Phosphorylation of PSD-95 Regulates Spine Morphogenesis Downstream of PAR-1—To examine the function of Ser-561 phosphorylation of PSD-95, we expressed non-phosphorylatable or phosphomimetic mutants of Ser-561 of PSD-95 in hippocampal neurons. First, we examined whether phosphorylation at Ser-561 regulates PSD-95 targeting to synapses. As shown in Fig. 4*a*, both mutants S561A and S561D localized well to synapses, similar to their wild-type counterpart. This shows that Ser-561 does not regulate synaptic targeting of PSD-95.

Next, we wanted to determine the role of Ser-561 phosphorylation in spine morphogenesis. To test this, we expressed either wild-type PSD-95 or the Ser-561 mutants in hippocampal neurons. Expression of wild-type PSD-95 or PSD-95(S561D) did not significantly affect the density of dendritic spines. Interestingly, however, the expression of the S561A mutant significantly reduced spine density (Fig. 4, *b* and *c*), suggesting that Ser-561 regulates spine morphogenesis.

Finally, we wanted to determine whether phosphorylation at Ser-561 is downstream of PAR-1 in regulating spine morphogenesis. We expressed kinase-dead PAR-1b(T175A,S179A) along with different PSD-95 constructs in hippocampal neurons. As shown in Fig. 5, only the S561D mutant was able to rescue the defect of kinase-dead PAR-1b, suggesting that PSD-95 Ser-561 phosphorylation is downstream of PAR-1 in spine morphogenesis. Taken together, these results show an important role for PAR-1 in dendritic spine morphogenesis through phosphorylating PSD-95 at Ser-561.

DISCUSSION

The morphogenesis and plasticity of dendritic spines play a key role in cognitive functions such as learning and memory.

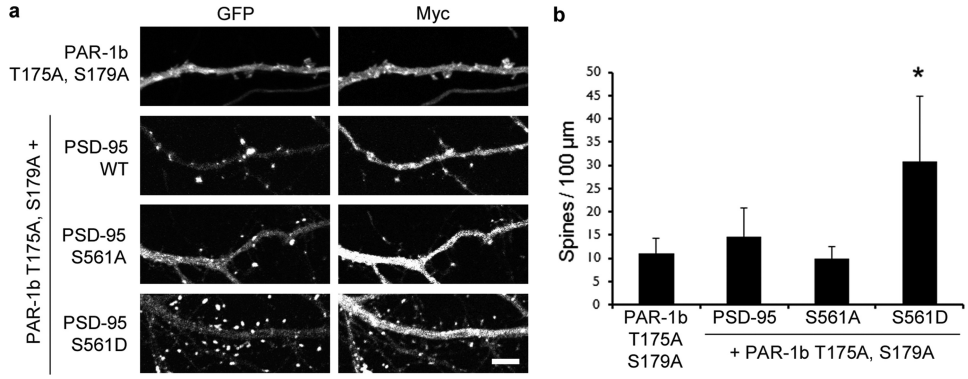

FIGURE 5. **Phosphomimetic mutant of PSD-95 rescues defects of kinase-dead PAR-1.** *a*, hippocampal neurons were cotransfected with PSD-95 constructs and the kinase-dead mutant PAR-1b(T175A,S179A). S561D, but not the other PSD-95 constructs, could rescue the defects of kinase-dead PAR-1. *Scale bar* = 5 μm. *b*, quantification of spine density in neurons shown in *a*. *, $p < 0.001$ by Student's *t* test. *Error bars* represent S.D. of the samples ($n \geq 83$ for each condition).

Thus, it is of central importance to understand the molecular mechanisms that regulate these processes. Our recent studies point to an important role for the PAR polarity proteins, including PAR-3 and the PAR-6·aPKC complex, in regulating this process. However, it is unclear whether and how other polarity proteins are involved. Here, we have shown that the polarity protein PAR-1 is important for normal dendritic spine morphogenesis in hippocampal neurons and that the kinase activity of PAR-1 is necessary for its effect. Consistent with our results, a recent study showed a role for MARK2/PAR-1b in spine maintenance (18). We have further shown that PAR-1 functions by phosphorylating the synaptic scaffolding protein PSD-95 at Ser-561. Phosphorylation at this site does not regulate PSD-95 targeting to synapses. However, it does regulate spine morphogenesis. Finally, we showed that a phosphomimetic mutant of PSD-95 was able to rescue the defects of kinase-dead PAR-1, suggesting that PSD-95 phosphorylation is downstream of PAR-1 in regulating spine morphogenesis.

Interestingly, overexpression of both kinase-active and kinase-dead PAR-1 causes a significant reduction in spine density. This suggests that a critical level of PAR-1 kinase activity is important for proper spine morphogenesis. This is consistent with previous studies in other systems, where either excessive PAR-1 activation or a reduction in PAR-1 activity caused polarity defects (19–21). It is unlikely that the effect of PAR-1 overexpression was due to downstream phosphorylation of PSD-95 because we observed no obvious spine defects in the PSD-95(S561D) mutant-expressing neurons. It is possible that overexpression of PAR-1 would cause hyperphosphorylation of the MAP tau. Hyperphosphorylation of tau would in turn cause a redistribution of tau from axons to the somatodendritic compartment and a decrease in spine density (22). Alternatively, although microtubule transport is not grossly affected by PAR-1 depletion, microtubule growth is regulated by PAR-1, as shown recently by Ohno and co-workers (18). Thus, it is possible that PAR-1 overexpression inhibits spine morphogenesis by affecting certain aspects of microtubule dynamics.

We have further shown that PAR-1 functions by phosphorylating PSD-95 on the conserved K*X*GS motif at Ser-561. In *Drosophila*, *Drosophila* dPAR-1 phosphorylates the PSD-95 homolog Dlg at the same conserved serine. Dlg phosphorylation by dPAR-1 has been shown to regulate its targeting to the neuromuscular junction (17). However, the phosphorylation of mammalian PSD-95 does not seem to affect its targeting to the postsynapse (Fig. 4*a*), which is consistent with previous studies showing that PSD-95 targeting is regulated by N-terminal palmitoylation, PDZ domains, and a targeting motif near the C terminus (23). Although phosphorylation at Ser-561 does not affect spine targeting of PSD-95, it does regulate spine morphogenesis. It will be of great interest to elucidate the mechanism by which Ser-561 phosphorylation regulates PSD-95 function.

Activity-dependent synaptic plasticity is believed to underlie learning and memory processes (24). Thus, it will be interesting to determine how PAR-1 is regulated by synaptic activity, which will shed light on whether and how PAR-1 is involved in higher order cognitive functions. This is especially important in light of the fact that PAR-1 has been implicated in the pathogenesis of both autism and Alzheimer disease (9, 11). Understanding the molecular pathways by which PAR-1 is involved in spine morphogenesis and synaptic plasticity will not only help us elucidate the basic mechanisms by which synapses are built but will also provide insight into the pathogenic processes involved in autism and Alzheimer disease.

Acknowledgments—We thank Drs. Ian Macara, Didier Trono (École Polytechnique Fédérale de Lausanne), Richard Youle, and Ann Marie Craig for reagents; Drs. Michael Matise and Mladen-Roko Rasin for access to the Syngene G:BOX iChemi XR system; and Dr. Stephen Moorman for access to the Leica DMRE microscope.

REFERENCES

1. Fiala, J. C., Spacek, J., and Harris, K. M. (2002) Dendritic spine pathology: cause or consequence of neurological disorders? *Brain Res. Brain Res. Rev.* **39,** 29–54
2. Penzes, P., Cahill, M. E., Jones, K. A., VanLeeuwen, J. E., and Woolfrey, K. M. (2011) Dendritic spine pathology in neuropsychiatric disorders. *Nat. Neurosci.* **14,** 285–293
3. Zhang, H., and Macara, I. G. (2006) The polarity protein PAR-3 and TIAM1 cooperate in dendritic spine morphogenesis. *Nat. Cell Biol.* **8,** 227–237
4. Zhang, H., and Macara, I. G. (2008) The PAR-6 polarity protein regulates dendritic spine morphogenesis through p190 RhoGAP and the Rho GTPase. *Dev. Cell* **14,** 216–226
5. Kemphues, K. J., Priess, J. R., Morton, D. G., and Cheng, N. S. (1988) Identification of genes required for cytoplasmic localization in early *C. el-*

egans embryos. *Cell* **52,** 311–320
6. Drewes, G., Ebneth, A., Preuss, U., Mandelkow, E. M., and Mandelkow, E. (1997) MARK, a novel family of protein kinases that phosphorylate microtubule-associated proteins and trigger microtubule disruption. *Cell* **89,** 297–308
7. Ebneth, A., Drewes, G., Mandelkow, E. M., and Mandelkow, E. (1999) Phosphorylation of MAP2c and MAP4 by MARK kinases leads to the destabilization of microtubules in cells. *Cell Motil. Cytoskeleton* **44,** 209–224
8. Goldstein, B., and Macara, I. G. (2007) The PAR proteins: fundamental players in animal cell polarization. *Dev. Cell* **13,** 609–622
9. Matenia, D., and Mandelkow, E. M. (2009) The tau of MARK: a polarized view of the cytoskeleton. *Trends Biochem. Sci.* **34,** 332–342
10. Segu, L., Pascaud, A., Costet, P., Darmon, M., and Buhot, M. C. (2008) Impairment of spatial learning and memory in ELKL motif kinase 1 (EMK1/MARK2) knock-out mice. *Neurobiol. Aging* **29,** 231–240
11. Maussion, G., Carayol, J., Lepagnol-Bestel, A. M., Tores, F., Loe-Mie, Y., Milbreta, U., Rousseau, F., Fontaine, K., Renaud, J., Moalic, J. M., Philippi, A., Chedotal, A., Gorwood, P., Ramoz, N., Hager, J., and Simonneau, M. (2008) Convergent evidence identifying MAP/microtubule affinity-regulating kinase 1 (MARK1) as a susceptibility gene for autism. *Hum. Mol. Genet.* **17,** 2541–2551
12. Wiznerowicz, M., and Trono, D. (2003) Conditional suppression of cellular genes: lentiviral vector-mediated drug-inducible RNA interference. *J. Virol.* **77,** 8957–8961
13. Karbowski, M., Arnoult, D., Chen, H., Chan, D. C., Smith, C. L., and Youle, R. J. (2004) Quantitation of mitochondrial dynamics by photolabeling of individual organelles shows that mitochondrial fusion is blocked during the Bax activation phase of apoptosis. *J. Cell Biol.* **164,** 493–499
14. Hurov, J. B., Watkins, J. L., and Piwnica-Worms, H. (2004) Atypical PKC phosphorylates PAR-1 kinases to regulate localization and activity. *Curr. Biol.* **14,** 736–741
15. Suzuki, A., Hirata, M., Kamimura, K., Maniwa, R., Yamanaka, T., Mizuno, K., Kishikawa, M., Hirose, H., Amano, Y., Izumi, N., Miwa, Y., and Ohno, S. (2004) aPKC acts upstream of PAR-1b in both the establishment and maintenance of mammalian epithelial polarity. *Curr. Biol.* **14,** 1425–1435
16. Mandelkow, E. M., Thies, E., Trinczek, B., Biernat, J., and Mandelkow, E. (2004) MARK/PAR-1 kinase is a regulator of microtubule-dependent transport in axons. *J. Cell Biol.* **167,** 99–110
17. Zhang, Y., Guo, H., Kwan, H., Wang, J. W., Kosek, J., and Lu, B. (2007) PAR-1 kinase phosphorylates Dlg and regulates its postsynaptic targeting at the *Drosophila* neuromuscular junction. *Neuron* **53,** 201–215
18. Hayashi, K., Suzuki, A., Hirai, S., Kurihara, Y., Hoogenraad, C. C., and Ohno, S. (2011) Maintenance of dendritic spine morphology by partitioning-defective 1b through regulation of microtubule growth. *J. Neurosci.* **31,** 12094–12103
19. Bayraktar, J., Zygmunt, D., and Carthew, R. W. (2006) PAR-1 kinase establishes cell polarity and functions in Notch signaling in the *Drosophila* embryo. *J. Cell Sci.* **119,** 711–721
20. Krahn, M. P., Egger-Adam, D., and Wodarz, A. (2009) PP2A antagonizes phosphorylation of Bazooka by PAR-1 to control apical-basal polarity in dividing embryonic neuroblasts. *Dev. Cell* **16,** 901–908
21. Nam, S. C., Mukhopadhyay, B., and Choi, K. W. (2007) Antagonistic functions of PAR-1 kinase and protein phosphatase 2A are required for localization of Bazooka and photoreceptor morphogenesis in *Drosophila*. *Dev. Biol.* **306,** 624–635
22. Jaworski, T., Lechat, B., Demedts, D., Gielis, L., Devijver, H., Borghgraef, P., Duimel, H., Verheyen, F., Kügler, S., and Van Leuven, F. (2011) Dendritic degeneration, neurovascular defects, and inflammation precede neuronal loss in a mouse model for tau-mediated neurodegeneration. *Am. J. Pathol.* **179,** 2001–2015
23. Craven, S. E., El-Husseini, A. E., and Bredt, D. S. (1999) Synaptic targeting of the postsynaptic density protein PSD-95 mediated by lipid and protein motifs. *Neuron* **22,** 497–509
24. Murakoshi, H., and Yasuda, R. (2012) Postsynaptic signaling during plasticity of dendritic spines. *Trends Neurosci.* **35,** 135–143